

## Total Cross-Sections for Reactions Induced by Oxygen-18 on Lithium

By TH. DIACO, C. FRIEDLI and P. LERCH\*, Institut d'Electrochimie et de Radiochimie, Swiss Federal Institute of Technology, CH-1015 Lausanne, Switzerland

(Received February 16, 1987)

*Nuclear reaction / Yield / Excitation function /  $^{18}\text{O}$  Particles / Target Li / Heavy ion activation*

### Abstract

In order to determine traces of lithium by Heavy Ion Activation Analysis (HIAA), the yield curves and the excitation functions for 9 nuclear reactions induced by  $^{18}\text{O}$  ions on  $^6\text{Li}$  and  $^7\text{Li}$ , were determined in the 10 to 40 MeV energy range. The best yields were obtained with the  $^7\text{Li}(^{18}\text{O}, \alpha n)^{20}\text{F}$  and the  $^6\text{Li}(^{18}\text{O}, 2\alpha)^{16}\text{N}$  reactions. The first reaction shows a maximum cross-section of  $1.02 \pm 0.09$  barn for a 26 MeV  $^{18}\text{O}$  ion beam, thus leading to a fast, non-destructive, selective and sensitive determination of traces of lithium.

### Introduction

The possibility of using an oxygen-18 ion beam for analytical purposes has been demonstrated in earlier papers [1–3]. Light elements, and particularly lithium, have shown an increasing role in the preparation of high purity material employed in advanced technology. It is one of the elements foreseen as the first wall material in fusion reactors [4] and its specific properties are useful in alloy- and glass preparation [5]. It appears, thus, justified to find out new sensitive analytical techniques for determining traces of this element.

In the present work, the excitation functions of nuclear reactions induced by bombarding both  $^6\text{Li}$  and  $^7\text{Li}$  isotopes with  $^{18}\text{O}$  particles have been established for a large energy range ( $E_{\text{lab}} = 10\text{--}40$  MeV) with the help of a cyclic irradiation-activity measurement set-up. Knowledge of the excitation functions of nuclear reactions is useful in order to find out the best experimental conditions for their analytical application. Furthermore, the short half-life radionuclides production allows a fast and non-destructive determination of trace elements if the cross-sections of the reaction of interest are large enough.

### Experimental

Beams of  $^{18}\text{O}$  ions at various energies and charge states were obtained with the HV EC-EN Tandem Van de Graaff accelerator of the Institute for Medium Energy Physics at the Swiss Federal Institute of Technology in Zürich. The  $^{18}\text{O}$  ions were obtained by sputtering of an enriched oxygen  $\text{Ca}^{18}\text{O}$  solid cone.

The targets were made of natural lithium oxide ( $\text{Li}_2\text{O}$ , p. a. MERCK AG, 92.5%  $^7\text{Li}$ ) and of enriched lithium oxide ( $^6\text{Li}_2\text{O}$ , Oak Ridge, 95%  $^6\text{Li}$ ). The powder was pressed in small discs of 15 mm diameter and 1–2 mm

thickness, weighing 200–300 mg. They were thicker than the range of the incident ion beam. The beam current on the target was kept below 25 nA in order to avoid sample damage and to maintain the dead time of the detector at a reasonably low level.

The experimental irradiation set-up, especially designed to determine the production yields of radionuclides with short half-lives, has been described in a earlier paper [6]. It allows cyclic irradiations and radioactivity measurements without interruption of vacuum ( $10^{-5}$  mm Hg). After an irradiation of typically 10 seconds, the mobile target holder was transferred to the counting position to be measured with a Ge(Li) detector (ORTEC 8001 1020V, 2.0 keV resolution at 1.33 MeV) through a thin plexiglass window for typically 30 seconds. The detector was linked to a multichannel analyzer (CANBERRA 80). The beam current was monitored immediately after the sample's activity measurement by using a Faraday cup placed directly behind the position of the irradiated target. The whole electronically controlled process (irradiation-activity measurement-beam monitoring) was repeated for 10 cycles at least. At the end of the final counting the total spectrum was transferred to a floppy disc recorder (SCIENTIFIC MICRO SYSTEM D 222) for further analysis with a PDP 11/23 computer. Standard  $^{152}\text{Eu}$  and  $^{22}\text{Na}$  sources with the same geometry as the targets were used for energy and efficiency calibration of the system.

### Cross-section calculation

Due to the cyclic mode and the summation of the consecutive spectra, the counting rate,  $a_0$ , at the end of the first irradiation had to be determined from the total number of counts,  $N_t$ , detected in the  $\gamma$ -line of the radionuclide of interest. The various adjustable experimental parameters, as optimized by a computer program [7], were taken into account.

$$a_0 = \frac{N_t \lambda (1 - e^{-\lambda t_c}) e^{\lambda t_D}}{(1 - e^{-\lambda \Delta t})(1 - e^{-\lambda t_i})} \left[ k + \frac{1 - e^{-\lambda k t_c}}{1 - e^{-\lambda t_c}} \right]^{-1}$$

where  $\lambda$  = decay constant ( $\text{s}^{-1}$ )

$t_c$  = time separating one irradiation from the next (s)

$t_D$  = delay between the end of irradiation and the beginning of counting (s)

$\Delta t$  = single counting time (s)

$t_i$  = single irradiation time (s)

$k$  = number of cycles

\* To whom correspondence should be addressed.

From this value, the reaction yield was determined for each incident energy, using the relation:

$$Y = \frac{a_0 t_i z}{6.24 \cdot 10^{12} (I t_i) \epsilon u} \quad (2)$$

where  $6.24 \cdot 10^{12}/z$  = beam current ( $I$ ) and ion flow interrelation factor

$z$  = number of charges of the incident ion

$I t_i$  = integrated charge collected on the target ( $\mu\text{C}$ )

$\epsilon$  = detector efficiency for the chosen  $\gamma$ -ray

$u$  = abundance of the  $\gamma$ -ray of interest [8]

The experimental activation curve obtained by reporting the yield as a function of the incident beam energy, was refined using a computer program [9]. The derivative of this latter curve,  $dY/dE$ , at a given beam energy led to the cross-section,  $\sigma(E)$ :

$$\sigma(E) = \frac{1}{n} \left( \frac{dY}{dE} \right)_E \left( \frac{dE}{dx} \right)_E \quad (3)$$

where  $n$  = concentration of atoms from which radionuclide of interest is formed (at  $\text{g}^{-1}$ )

$\frac{dE}{dx}$  = differential energy loss of the incident ions ( $\text{MeV g}^{-1} \text{cm}^2$ ) given by ZIEGLER [10]

## Results and discussion

A list of nuclear reactions induced by bombarding lithium with an  $^{18}\text{O}$  ion beam was established. Taken into account were those which led to the production of a radionuclide and to the emission of simple particles ( $n$ ,  $^1\text{H}$ ,  $^2\text{H}$ ,  $^3\text{H}$ ,  $^3\text{He}$ ,  $^4\text{He}$ ). They are presented in Table 1, together with the  $Q$ -values, the Coulomb barriers and the nuclear characteristics of the radioactive products. Apart of the  $^6\text{Li}(^{18}\text{O}, ^3\text{He})^{21}\text{F}$  reaction, all the reactions are exoenergetic and their Coulomb barriers are relatively low. Almost all of the products have short half-lives ( $T_{1/2} < 200$  s). This fact presents an interesting feature for anal-

**Table 1.** Reactions induced by  $^{18}\text{O}$  ions on lithium and nuclear characteristics

Reaction	$Q$ -value (MeV)	Coulomb barrier (MeV)	Produced radionuclide	
			$T_{1/2}$	$E_\gamma$ (keV)
$^6\text{Li}(^{18}\text{O}, p)^{23}\text{Ne}$	11.2	20.8	38.0 s	440
$^6\text{Li}(^{18}\text{O}, \alpha)^{20}\text{F}$	10.9		11.4 s	1634
$^6\text{Li}(^{18}\text{O}, 2\alpha)^{16}\text{N}$	2.7		7.1 s	6128
$^6\text{Li}(^{18}\text{O}, ^3\text{He})^{21}\text{F}$	-1.6		4.3 s	351
$^7\text{Li}(^{18}\text{O}, n)^{24}\text{Na}$	14.5	18.2	15.0 h	1369
$^7\text{Li}(^{18}\text{O}, p)^{24}\text{Ne}$	12.8		202.8 s	472
$^7\text{Li}(^{18}\text{O}, d)^{23}\text{Ne}$	6.1		38.0 s	440
$^7\text{Li}(^{18}\text{O}, \alpha)^{21}\text{F}$	11.8		4.3 s	351
$^7\text{Li}(^{18}\text{O}, \alpha n)^{20}\text{F}$	2.8		11.4 s	1634
$^7\text{Li}(^{18}\text{O}, p\alpha)^{20}\text{O}$	0.6		13.6 s	1057

tical applications. Indeed, the reaction of interest could lead to fast and non-destructive lithium determination, as the difficulties of dealing with short half-life radioisotopes have been resolved by using a cyclic activation technique.

Figures 1 and 2 show typical spectra obtained by irradiating both lithium oxide samples with a 25 MeV  $^{18}\text{O}^{+4}$  beam. In Figure 1, the gain of the counting system was set to get the first part of the spectrum (100–4000 keV). All the predicted radionuclides can be seen. Moreover, the  $^{19}\text{O}$  was produced by the  $^6\text{Li}(^{18}\text{O}, p\alpha)^{19}\text{O}$  reaction which has been already studied (3) as an interfering reaction to the determination of trace beryllium. Both aluminum radioisotopes ( $^{28}\text{Al}$  at 1779 keV and  $^{29}\text{Al}$  at 1273 keV) are probably due to reactions with the oxygen of the  $\text{Li}_2\text{O}$  targets:  $^{16}\text{O}(^{18}\text{O}, ^6\text{Li})^{28}\text{Al}$  and  $^{16}\text{O}(^{18}\text{O}, ^5\text{Li})^{29}\text{Al}$ . Furthermore,  $^{24}\text{Na}$  cannot be seen because of the short irradiation time; its production yield and reaction cross-section will not be discussed in this paper. Figure 2 shows the spectra obtained when setting the gain of the counting system with an upper limit of 10 MeV. In the case of the enriched  $^6\text{Li}$  target, the  $\gamma$ -lines of  $^{16}\text{N}$  are well visible.

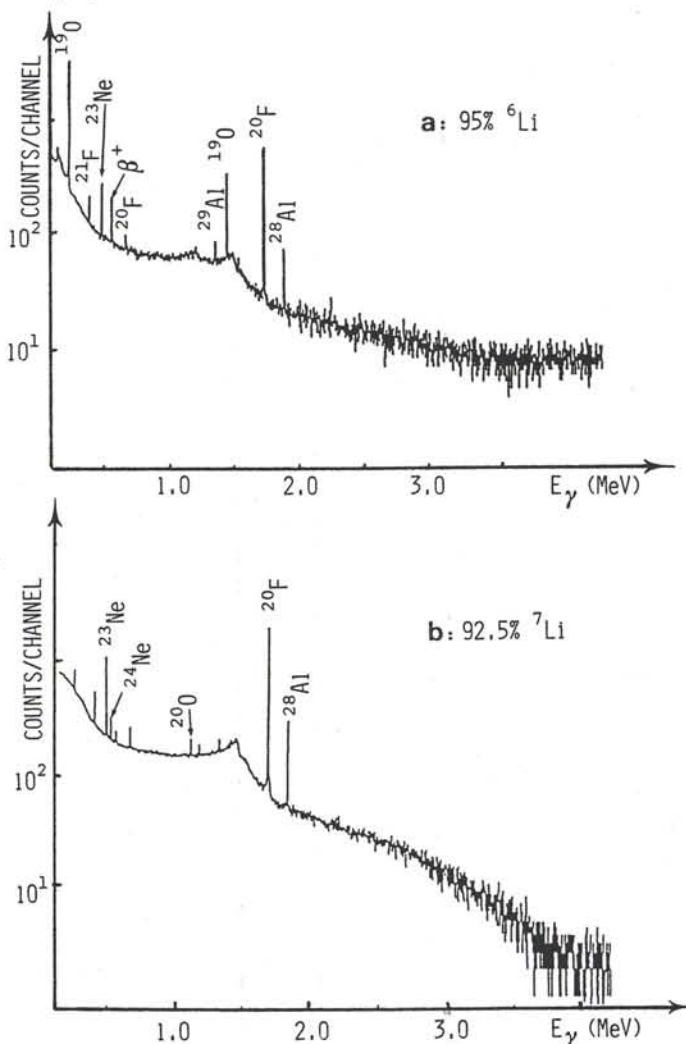


**Fig. 1.** Spectra of  $\text{Li}_2\text{O}$  targets irradiated with 25 MeV  $^{18}\text{O}^{+4}$  ions:  $\gamma$ -energy range, 100–4000 keV.

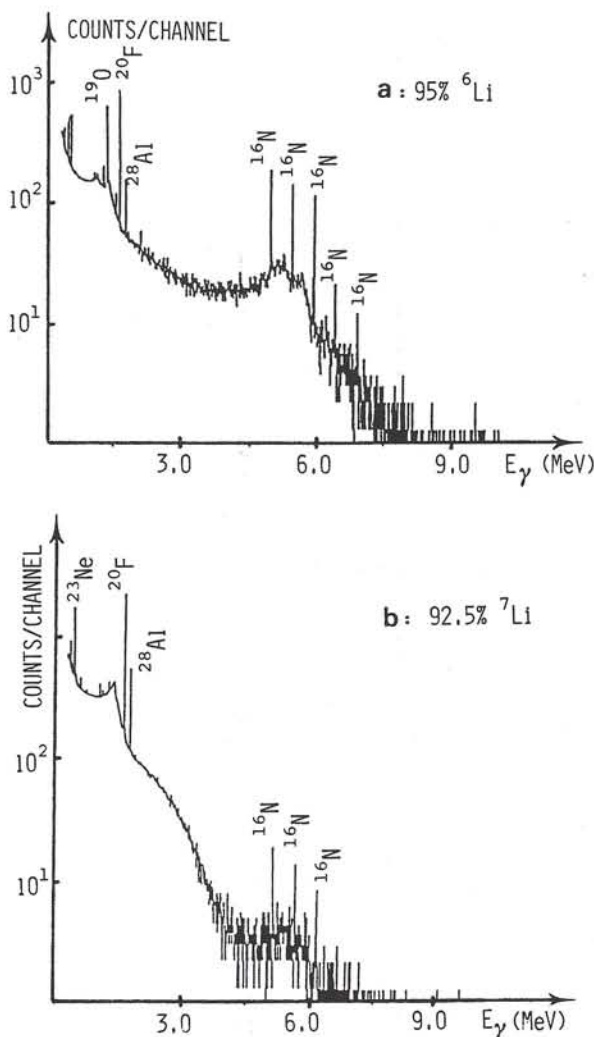


Fig. 2. Spectra of  $\text{Li}_2\text{O}$  targets irradiated with 25 MeV  $^{18}\text{O}^{4+}$  ions:  $\gamma$ -energy range, 0.5–10 MeV.

In order to determine the contribution of both  $^6\text{Li}$  and  $^7\text{Li}$  to the production of the various detected radionuclides, the  $^6\text{Li}_2\text{O}$  and  $^7\text{Li}_2\text{O}$  targets were systematically irradiated with  $^{18}\text{O}$  beams. All the reactions were studied between  $E_{\text{lab}} = 10$  MeV and  $E_{\text{lab}} = 40$  MeV  $^{18}\text{O}$ . The charge state of the  $^{18}\text{O}$  ions increased from +3 to +6 upon increasing the beam energy.

Table 2 presents the relative contributions of  $^6\text{Li}$  and  $^7\text{Li}$  to the production of each radionuclide. They are expressed as the percentage of the total specific activity measured at a given  $^{18}\text{O}$  energy. The abundance of  $^6\text{Li}$  and  $^7\text{Li}$  in both types of targets were taken into account. From these calculations, it appears that:

- $^{16}\text{N}$  is only produced by the  $^6\text{Li}(^{18}\text{O}, 2\alpha)^{16}\text{N}$  reaction;
- $^{24}\text{Ne}$  and  $^{20}\text{O}$  are only produced by reactions with  $^7\text{Li}$ ;
- the contribution of  $^6\text{Li}$  and  $^7\text{Li}$  reactions to the production of  $^{20}\text{F}$  and  $^{23}\text{Ne}$  is constant whatever the incident beam energy;
- the contribution of  $^6\text{Li}$  and  $^7\text{Li}$  reactions to the production of  $^{21}\text{F}$  varies with the beam energy.

Table 2. Contribution (%) of  $^6\text{Li}$  and  $^7\text{Li}$  to the production of the various radionuclides as a function of the beam energy

Radionuclide	Isotope	Beam energy (MeV)							Average
		10	15	20	25	30	35	40	
$^{16}\text{N}$	$^6\text{Li}$	0	100	100	100	100	100	100	
	$^7\text{Li}$	0	0	0	0	0	0	0	
$^{20}\text{O}$	$^6\text{Li}$	0	0	0	0	0	0	0	
	$^7\text{Li}$	0	0	100	100	100	100	100	
$^{20}\text{F}$	$^6\text{Li}$	12	9	13	11	12	13	14	$12.0 \pm 1.8$
	$^7\text{Li}$	88	91	87	89	88	87	86	$88.0 \pm 1.8$
$^{21}\text{F}$	$^6\text{Li}$	0	0	6	11	29	32	46	
	$^7\text{Li}$	0	100	94	89	71	68	54	
$^{23}\text{Ne}$	$^6\text{Li}$	0	7	8	6	9	9	9	$8.0 \pm 1.3$
	$^7\text{Li}$	0	93	92	94	91	91	91	$92.0 \pm 1.3$
$^{24}\text{Ne}$	$^6\text{Li}$	0	0	0	0	0	0	0	
	$^7\text{Li}$	0	100	100	100	100	100	100	

The knowledge of these contributions allowed the yield curves to be determined and the excitation functions to be established for all the reactions studied here.

#### Excitation functions for the reactions with $^6\text{Li}$

The yield of the reactions at a given  $^{18}\text{O}$  energy has been calculated for the detected radionuclides. They are expressed as  $\text{Bq} \cdot \text{ion}^{-1} \cdot \text{s}$  corresponding to the number of disintegrations per incident ion. The yield curves are given in Figure 3; in order to present them on the same graph, the yields scale is logarithmic. On a linear base, the curve show inflexion points for the reactions producing  $^{20}\text{F}$ ,  $^{21}\text{F}$  and  $^{23}\text{Ne}$ . The latter even reaches a plateau at about 38 MeV  $^{18}\text{O}$ . Only the yield for the  $^6\text{Li}(^{18}\text{O}, 2\alpha)^{16}\text{N}$  reaction is monotonically increasing throughout the whole energy range. The errors on  $Y(E)$  have been estimated to range between 6% and 12% depending on the reaction studied.

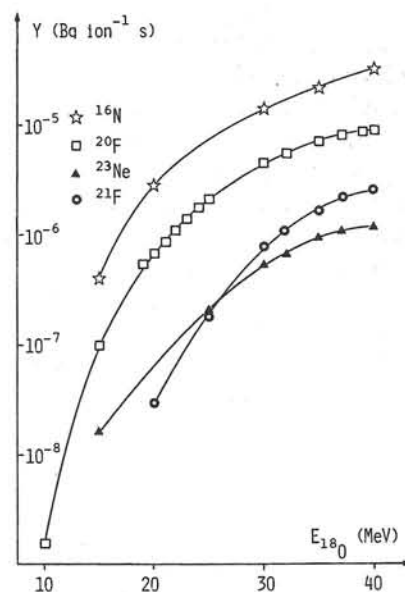


Fig. 3. Yield curves.  $^6\text{Li} + ^{18}\text{O}$  reactions.



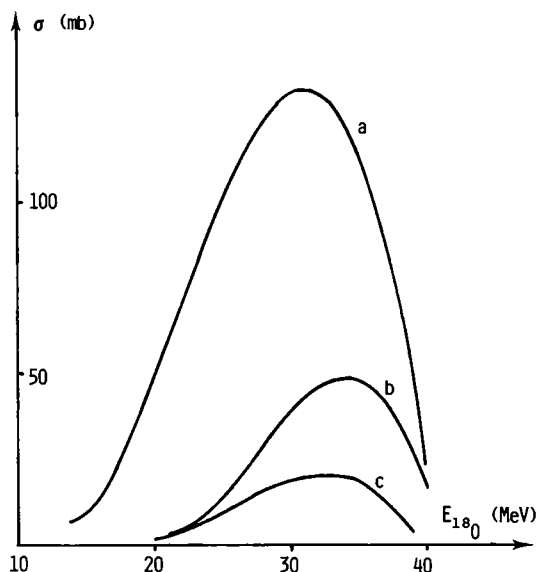


Fig. 4. Excitation functions for the reactions a)  ${}^6\text{Li}({}^{18}\text{O}, \alpha){}^{20}\text{F}$ , b)  ${}^6\text{Li}({}^{18}\text{O}, {}^3\text{He}){}^{21}\text{F}$ , c)  ${}^6\text{Li}({}^{18}\text{O}, p){}^{23}\text{Ne}$ .

Table 3. Maximum cross-sections for the reactions with  ${}^6\text{Li}$  and  ${}^7\text{Li}$

Reaction	Energy (MeV)	Cross-section (mb)
${}^6\text{Li}({}^{18}\text{O}, 2\alpha){}^{16}\text{N}$	40	$470 \pm 90$ a)
${}^6\text{Li}({}^{18}\text{O}, \alpha){}^{20}\text{F}$	31	$130 \pm 20$
${}^6\text{Li}({}^{18}\text{O}, {}^3\text{He}){}^{21}\text{F}$	34	$50 \pm 6$
${}^6\text{Li}({}^{18}\text{O}, p){}^{23}\text{Ne}$	32	$20 \pm 2$
${}^7\text{Li}({}^{18}\text{O}, \alpha n){}^{20}\text{F}$	26	$1020 \pm 90$
${}^7\text{Li}({}^{18}\text{O}, d){}^{23}\text{Ne}$	26	$160 \pm 15$
${}^7\text{Li}({}^{18}\text{O}, \alpha){}^{21}\text{F}$	31	$60 \pm 5$
${}^7\text{Li}({}^{18}\text{O}, p\alpha){}^{20}\text{O}$	40	$9 \pm 1.5$ a)
${}^7\text{Li}({}^{18}\text{O}, p){}^{24}\text{Ne}$	15	$7 \pm 2$ b)

a) Cross-sections still increasing beyond 40 MeV  ${}^{18}\text{O}$ .

b) cross-sections continuously decreasing throughout the energy range.

The excitation functions were determined using these data; they are presented in Figures 4 and 7. For the  ${}^6\text{Li}({}^{18}\text{O}, \alpha){}^{20}\text{F}$ ,  ${}^6\text{Li}({}^{18}\text{O}, {}^3\text{He}){}^{21}\text{F}$  and  ${}^6\text{Li}({}^{18}\text{O}, p){}^{23}\text{Ne}$  reactions, the functions reach a maximum cross-section value reported in Table 3. The  ${}^6\text{Li}({}^{18}\text{O}, 2\alpha){}^{16}\text{N}$  reaction leads to the highest cross-sections (Fig. 7). The produced  ${}^{16}\text{N}$  yields very high energy  $\gamma$ -rays (5–7 MeV) which for the efficiency of the Ge(Li) detector is difficult to know precisely. SEYFART *et al.* [11], however, have studied the efficiency of standard type Ge(Li) detectors for high energy  $\gamma$ -rays. Based on this work, the efficiency of our detector was evaluated to be  $(3.5 \pm 0.1) \cdot 10^{-4}$  at 6128 keV. Due to the lack of accuracy in determining this value, the errors on the cross-sections for this reaction were estimated to be 40%. For the 3 other reactions, the errors remain lower than 25%.

Excitation functions for the reactions with  ${}^7\text{Li}$

The yield curves of the 5 reactions studied with  ${}^7\text{Li}$  are presented in Figure 5. Again, due to the large differences

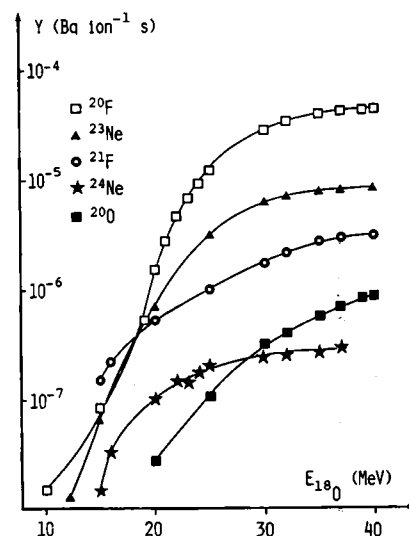


Fig. 5. Yield curves.  ${}^7\text{Li} + {}^{18}\text{O}$  reactions

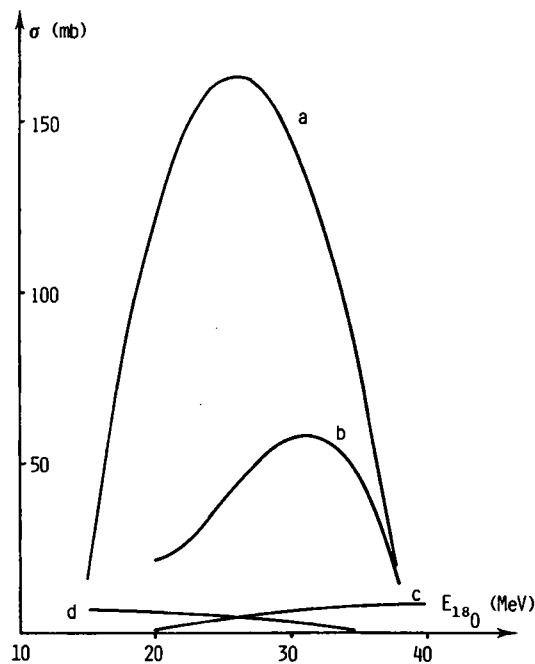


Fig. 6. Excitation functions for the reactions a)  ${}^7\text{Li}({}^{18}\text{O}, d){}^{23}\text{Ne}$ , b)  ${}^7\text{Li}({}^{18}\text{O}, \alpha){}^{21}\text{F}$ , c)  ${}^7\text{Li}({}^{18}\text{O}, p\alpha){}^{20}\text{O}$ , d)  ${}^7\text{Li}({}^{18}\text{O}, p){}^{24}\text{Ne}$ .

between the values obtained, a logarithmic yields scale has been chosen. The yields obtained with the  ${}^7\text{Li}({}^{18}\text{O}, \alpha n){}^{20}\text{F}$  reaction are the highest of all the nuclear reactions for most of the  ${}^{18}\text{O}$  beam energies; at 40 MeV, its value reaches  $(4.3 \pm 0.1) \cdot 10^{-5} \text{ Bq} \cdot \text{ion}^{-1} \cdot \text{s}$ . The reactions producing  ${}^{20}\text{F}$ ,  ${}^{23}\text{Ne}$  and  ${}^{21}\text{F}$  show inflexion points and reach plateaus at about 35 MeV. The  ${}^7\text{Li}({}^{18}\text{O}, p\alpha){}^{20}\text{O}$  and  ${}^7\text{Li}({}^{18}\text{O}, p){}^{24}\text{Ne}$  reactions are still smoothly increasing at 40 MeV. The yield values for these two latter reactions remain low:  $(9.2 \pm 0.8) \cdot 10^{-7} \text{ Bq} \cdot \text{ion}^{-1} \cdot \text{s}$  for the production of  ${}^{20}\text{O}$  and  $(3.2 \pm 0.6) \cdot 10^{-7} \text{ Bq} \cdot \text{ion}^{-1} \cdot \text{s}$  for the  ${}^7\text{Li}({}^{18}\text{O}, p){}^{24}\text{Ne}$  reaction.

The corresponding excitation functions are presented in Figures 6 and 7. As forseen, the functions for the  ${}^7\text{Li}({}^{18}\text{O}, \alpha n){}^{20}\text{F}$  (Fig. 7),  ${}^7\text{Li}({}^{18}\text{O}, d){}^{23}\text{Ne}$  and

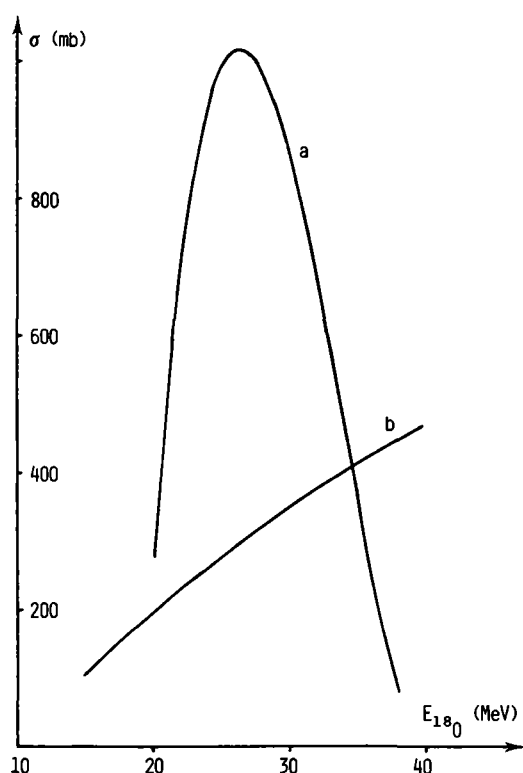


Fig. 7. Excitation functions for the reactions a)  ${}^7\text{Li}({}^{18}\text{O}, \alpha){}^{20}\text{F}$ , b)  ${}^6\text{Li}({}^{18}\text{O}, 2\alpha){}^{16}\text{N}$ .

${}^7\text{Li}({}^{18}\text{O}, \alpha){}^{20}\text{F}$  reactions reach maximum cross-section values, given in Table 3, with errors of about 15%. The two other reactions have very low cross-sections and the values given here are only qualitative because of the lack of precision in measuring the activities of  ${}^{20}\text{O}$  and  ${}^{24}\text{Ne}$ .

## Conclusion

In the point of view of an analytical application, the cross-sections for both  ${}^6\text{Li}({}^{18}\text{O}, 2\alpha){}^{16}\text{N}$  and  ${}^7\text{Li}({}^{18}\text{O}, \alpha){}^{20}\text{F}$  reactions are large enough to be utilized for the determination of lithium. Due to the small natural abundance of  ${}^6\text{Li}$ , the first one leads, however, to poor sensitivities. Its application can be considered because of the very low background recorded in the high energy  $\gamma$ -ray region where  ${}^{16}\text{N}$  is detected.

On the other hand, the second reaction can be applied to lithium trace determination. The detection limit for lithium has been calculated to be 2 ng when using a cyclic activation analysis device and a 40 MeV, 100 nA  ${}^{18}\text{O}^{+6}$  ion beam. The selectivity of this reaction has been checked

by irradiating a series of elements likely to produce  ${}^{20}\text{F}$ . Among the 9 elements suspected for nuclear interference, as identified with a computer program [12], only boron showed an interference of 5% compared to the activity produced from lithium. At 40 MeV, nitrogen, fluoride and sodium also interfere but their contribution to the production of  ${}^{20}\text{F}$  remains smaller than 0.5%.

Thus a fast, non-destructive, selective and sensitive determination of lithium is possible. The technique has already been applied successfully to NBS glass samples which contain up to 60 trace elements.

## Acknowledgement

The assistance of the Tandem Van de Graaff accelerator personnel is gratefully acknowledged.

## Literature

1. DIACO, TH., FRIEDLI, C., LERCH, P.: Excitation Functions for the  ${}^9\text{Be}({}^{18}\text{O}, 2\alpha){}^{19}\text{O}$  and  ${}^9\text{Be}({}^{18}\text{O}, d){}^{25}\text{Na}$  Reactions. *Radiochim. Acta* **38**, 185 (1985).
2. DIACO, TH., FRIEDLI, C., LERCH, P.: Trace Determination of Beryllium by Radioactivation in an Oxygen-18 Ion Beam. *Proc. 5th Intn'l Conf. on Nuclear Methods in Environmental and Energy Research*, CONF-840408, University of Missouri 1984, p. 699.
3. FRIEDLI, C., DIACO, TH., LERCH, P.: Lithium and Beryllium Trace Determination Using Heavy Ion Activation Analysis. *Proc. 7th Intn'l Conf. on Modern Trends in Activation Analysis*, Copenhagen 1986, p. 327.
4. PROFIO, A. E.: *Radiation Shielding and Dosimetry*. J. Wiley & Sons, New York 1979, p. 486.
5. HART, W. A., BEUMEL, O. F. JR.: *Lithium*. In *Comprehensive Inorganic Chemistry* (J. C. BAILAR et al., ed.), Vol. I, Pergamon Press, Oxford 1973, p. 339.
6. FRIEDLI, C., ROUSSEAU, M., DIACO, TH., LERCH, P.: Dosage de traces de soufre et de béryllium par activation dans un faisceau d'oxygène-18. *Analisis* **13**, 176 (1985).
7. COLIN, M., FRIEDLI, C., LERCH, P.: Heavy Ion Activation Analysis: Theoretical Approach for Optimizing Cyclic Analysis. *Nucl. Instr. Meth. Phys. Res. B* **10/11**, 1062 (1985).
8. ERDTMANN, G., SOYKA, W.: *The Gamma Rays of Radionuclides. Topical Presentation in Nuclear Chemistry*, Vol. 7, Verlag Chemie, Weinheim 1979.
9. GOUMAZ, J. Y., DURAND, C., OTTIN, T.: Programme FIDES, LTA-GRH Report 14B, EPF-Lausanne 1983.
10. ZIEGLER, J. F.: *Handbook of Stopping Cross-Sections for Energetic Ions in all Elements*, Vol. 5, Pergamon Press, New York 1980.
11. SEYFARTH, H., HASSAN, A. M., HRASNIK, B., GOETTEL, P., DALANG, W.: Efficiency Determination for some Standard Type Ge(Li) Detectors for Gamma-Rays in the Energy Range from 0.04 to 11 MeV. *Nucl. Instr. Meth.* **105**, 301 (1972).
12. BARROS-LEITE, C. V., SCHWEIKERT, E. A.: Studies in Heavy Ion Activation Analysis, I. On the Selection of Activation Reactions, *J. Radioanal. Chem.* **53**, 173 (1979).

